Supporting Information of

Two-dimensional microfluidic system for the simultaneous quantitative analysis of phototactic/chemotactic responses of microalgae

Young Joon Sung[1,†], Ho Seok Kwak[2,†], Min Eui Hong[1], Hong Il Choi[1] and Sang Jun Sim[1,*]

[1]Department of Chemical and Biological Engineering, Korea University, 145, Anam-ro, Seongbuk-gu, Seoul 02841, Republic of Korea
[2]Department of Food Engineering, Dongyang Mirae University, 445, Gyeongin-ro, Guro-gu, Seoul, 08221, Republic of Korea

[†]These authors contributed equally to this work.
*Corresponding author: Professor Sang Jun Sim
Tel: +82-2-3290-4853
Fax: +82-2-926-6102
E-mail: simsj@korea.ac.kr

Abstract. Cell performance data and cell distribution histogram of 14 mutant strains and wild type strain were provided. Screening process using this platform was described in detail. Finally, cell distribution data in the outlet chambers with different chemotactic response to HCO_3^- during 5 consecutive screenings were provided.

Contents

Online Methods

Fabrication of microfluidic device

A microfluidic device design was created using AutoCAD software and printed on photomask film. We fabricated a silicon mold using SU-8 negative photoresist (SU-8 50, MicroChem Corp., Westborough, MA) on silicon wafers. The polydimethylsiloxane (PDMS) prepolymer (10:1 mixture of 184 Sylgard base and curing agent; Dow Corning, Midland, MI) was poured on the SU-8 mold and cured thermally at 80 °C. The PDMS layer containing the microchannel was bonded to a glass slide using oxygen plasma. The microfluidic device with flow channels was washed with 70% ethanol solution and irradiated with ultraviolet (UV) light to prevent contamination.

Injection of microalgae into the microfluidic device

The developed microfluidic device consists of 1 inlet, 8 outlets, cell migration channel, chemical source reservoir, and sink. To maintain the hydrostatic balance in the microfluidics, all microfluidic channels were filled with medium up to 10 mm of liquid height. For the injection of microalgae, a 40 μL of medium was removed from the inlet of the microfluidic device. Then, the same volume of cell suspension was carefully loaded into the inlet using a micropipette. The total volume of the solution filled in the microfluidic channel can be calculated as approximately 3,719.81 μL (Table S-1). The 40 μL of cell suspension loaded into the inlet of microfluidics is only 1.08% of the total solution volume in the microfluidic channels, and thus would not have a significant effect on the overall hydrostatic balance and generate chemical gradient in the microfluidics. In particular, since the injection of microalgae was carried out within 5 seconds using a micropipette, the chemical gradient in the microfluidic device was unlikely to be destroyed. The consistency in the chemical gradient was confirmed by the change of concentration gradients of fluorescein near the inlet and cell migration channel (Figure S-1).

Calculation of phototaxis index (PI) and chemotaxis index (CI)

The PI was defined as follows:

$$\mathrm{PI}(x) = \sum_{i=1}^{8}(n_i)\,/N_i \tag{1}$$

where n_i is the number of cells counted at each outlet chamber in response to light stimulus for 30 min ($i = 1, 2, 3, \cdots, 8$), and N_i is the initial number of cells in the inlet chamber. PI = 1 indicates that all cells in the inlet chamber moved toward the outlet chambers by phototaxis, and PI = 0 indicates that there were no cells observed in the outlet chambers after 30 min of illumination. The CI was defined as follows:

$$\mathrm{CI}(x) = \sum_{i=1}^{8}(c_i \times n_i) \,/\, \sum_{i=1}^{8} n_i \tag{2}$$

where c_i is the ratio of chemical concentration in each outlet chamber to the chemical concentration in the chemical source reservoir, and n_i is the number of cells in each outlet chamber ($i = 1, 2, 3, \cdots, 8$). CI = 1 indicates that all cells moved toward the chemical source reservoir (i.e. a high chemical concentration), and CI = 0 indicates that all cells moved away from the chemical source reservoir.

Measurements of Photosystem II (PSII) operating efficiency and CO_2 fixation rate

Chlorophyll fluorescence was measured with an FMS2 portable fluorometer (Hansatech Instruments, Pentney, UK) to determine cell growth. Cells at exponential phase (30 μg of chlorophyll a) were loaded onto a glass-fiber filter, and the filter was placed on the leaf clip of the fluorometer. For determination of the PSII operating efficiency, Y(II), cells (without dark-adaptation) were exposed to stepwise-increasing actinic light (from 1 to 900 μmol photons m^{-2} s^{-1}) for 20 s at each light intensity, and a saturating flash (3,000 μmol photons m^{-2} s^{-1}, 0.7 s duration) was applied to measure Fm' (maximum fluorescence). Y(II) was calculated as (Fm'–Fs)/Fm'. The CO_2 fixation rate of microalgae was determined from the carbon content of algal cells and the growth rate by equation (3):[1]

$$R_{CO_2} = C_C \times \mu_M \times \left(\frac{M_{CO_2}}{M_C}\right) \quad (3)$$

where R_{CO_2} is the CO_2 fixation rate (g L^{-1} day^{-1}) and C_C is the ratio of carbon content in algal biomass as measured by an elemental analyzer (Thermo Fisher Scientific, Waltham, MA). In addition, μ_M is the maximum growth rate (g L^{-1} day^{-1}) which was calculated using the Gompertz equation[2] with SigmaPlot 10.0 (Systat Software, Inc., San Jose, CA). M_{CO_2} and M_C represent the molecular weight of CO_2 and elemental carbon, respectively.

Calculation of preferred chemical source concentration for different microalgal strains

The concentration of HCO_3^- preferred by different microalgal strains could be determined by comparing the calculated HCO_3^- concentrations and the number of cells that reached the outlet chambers. More specifically, the preferred HCO_3^- concentration for each microalgae strain is the HCO_3^- concentration of the outlet chamber where the microalgae cells reach on average. Therefore, based on the distribution of microalgae cells reaching the outlet chambers by the chemotaxis, the average value of the preferred HCO_3^- concentration can be calculated as follows.

$$C = \sum_{i=1}^{8} x_i p_i$$ (where, C: preferred HCO_3^- concentration of cells, x_i = HCO_3^- concentration in outlet chamber, p_i = Fraction of responded cells)

In Table S-2, the preferred concentrations of HCO_3^- for *Chlamydomonas reinhardtii* CC125 was calculated.

Screening process to increase the separation efficiency

To increase the separation efficiency, a 40 μL of cell suspension taken from a specific outlet chamber (C1 or C8) at the previous screening step was transferred to the inlet chamber of the microfluidic chip at the next screening step. There was difference in the number of cells reaching a certain outlet chamber (C1 or C8) and the number of cells reaching all outlet chambers (C1 to C8). The reason for this difference might be the error in the cell count and the cell loss in the process of transferring the cell suspension.

Table S-1. Volume of the solution filled in the all microfluidic channels and structures.

	Width/diameter (mm)	Length (mm)	Height (mm)	# of parts	Volume (μL)
Inlet	4	-	10	1	125.66
Outlets	1	-	10	8	62.83
Cell migration channel	20	40	0.1	1	80.00
Chemical source reservoir	4	40	10	1	1725.66
Sink	4	40	10	1	1725.66
Total	-	-	-	-	**3719.81**

* Inlet and Outlets: 1 circle

* Cell migration channel: 1 rectangle

* Chemical source reservoir and Sink: 1 rectangle + 1 circle

Table S-2. Calculated HCO_3^- concentrations, distribution of microalgae cells reaching the outlet chambers, and preferred concentrations of HCO_3^- for *Chlamydomonas reinhardtii* CC125.

	HCO_3^- conc. (mM)		Cell distribution (%)		Preferred conc. (mM)	
Loading	70	200	70	200	70	200
Outlet 8	64.91 ± 3.25	185.47 ± 9.27	8.94 ± 0.30	0.68 ± 0.21		
Outlet 7	41.03 ± 2.05	117.24 ± 5.86	12.98 ± 1.96	4.19 ± 0.39		
Outlet 6	24.85 ± 1.24	71.01 ± 3.55	15.74 ± 1.48	7.25 ± 1.33		
Outlet 5	15.90 ± 0.79	45.43 ± 2.27	18.42 ± 1.28	11.86 ± 0.88		
Outlet 4	10.17 ± 0.51	29.05 ± 1.45	17.86 ± 1.54	17.61 ± 1.24	21.65 ± 4.18	32.79 ± 6.42
Outlet 3	8.15 ± 0.41	23.30 ± 1.16	11.45 ± 0.68	19.89 ± 0.21		
Outlet 2	6.44 ± 0.32	18.40 ± 0.92	8.37 ± 0.91	19.88 ± 0.72		
Outlet 1	4.71 ± 0.24	13.47 ± 0.67	6.22 ± 0.80	18.63 ± 1.29		
Sum	-	-	100.00	100.00		
Average	-	-	-	-	**27.22 ± 5.30**	

Table S-3. PSII operating efficiency, maximum growth rates, carbon content, and CO_2 fixation rates of 14 mutant strains and wild type (WT) strain (CC125).

Strains	Phototaxis index	Chemotaxis index	PSII operating efficiency, Y(II)	Maximum growth rate, μ_{max} (g L^{-1} day^{-1})	Carbon contents, C_C (%)	Carbon dioxide fixation rate, R_{CO2} (g L^{-1} day^{-1})
WT (CC125)	0.393 ± 0.035	0.332 ± 0.029	0.649 ± 0.001	0.395 ± 0.001	44.6 ± 0.04	0.645 ± 0.002
M1	0.374 ± 0.046	0.290 ± 0.048	0.630 ± 0.002	0.370 ± 0.003	44.1 ± 0.08	0.598 ± 0.001
M2	0.480 ± 0.059	0.526 ± 0.065	0.671 ± 0.005	0.436 ± 0.002	44.9 ± 0.05	0.717 ± 0.002
M3	0.635 ± 0.078	0.600 ± 0.035	0.704 ± 0.006	0.445 ± 0.005	46.4 ± 0.07	0.757 ± 0.001
M4	0.468 ± 0.058	0.506 ± 0.062	0.671 ± 0.005	0.433 ± 0.005	45.1 ± 0.05	0.715 ± 0.001
M5	0.400 ± 0.049	0.511 ± 0.035	0.652 ± 0.001	0.429 ± 0.002	44.7 ± 0.06	0.704 ± 0.006
M6	0.262 ± 0.032	0.241 ± 0.030	0.590 ± 0.005	0.326 ± 0.005	43.1 ± 0.09	0.515 ± 0.003
M7	0.381 ± 0.047	0.346 ± 0.035	0.637 ± 0.005	0.372 ± 0.002	44.4 ± 0.06	0.605 ± 0.002
M8	0.500 ± 0.061	0.632 ± 0.078	0.694 ± 0.001	0.454 ± 0.003	45.8 ± 0.08	0.763 ± 0.006
M9	0.396 ± 0.028	0.544 ± 0.038	0.649 ± 0.006	0.411 ± 0.002	44.7 ± 0.04	0.673 ± 0.009
M10	0.368 ± 0.026	0.221 ± 0.015	0.629 ± 0.001	0.361 ± 0.001	43.4 ± 0.07	0.575 ± 0.002
M11	0.381 ± 0.047	0.295 ± 0.036	0.632 ± 0.009	0.370 ± 0.007	44.4 ± 0.11	0.602 ± 0.007
M12	0.381 ± 0.047	0.540 ± 0.036	0.640 ± 0.003	0.407 ± 0.001	44.6 ± 0.07	0.664 ± 0.006
M13	0.523 ± 0.064	0.621 ± 0.076	0.684 ± 0.003	0.426 ± 0.002	45.3 ± 0.03	0.707 ± 0.002
M14	0.304 ± 0.037	0.211 ± 0.026	0.611 ± 0.005	0.342 ± 0.005	43.2 ± 0.03	0.541 ± 0.004

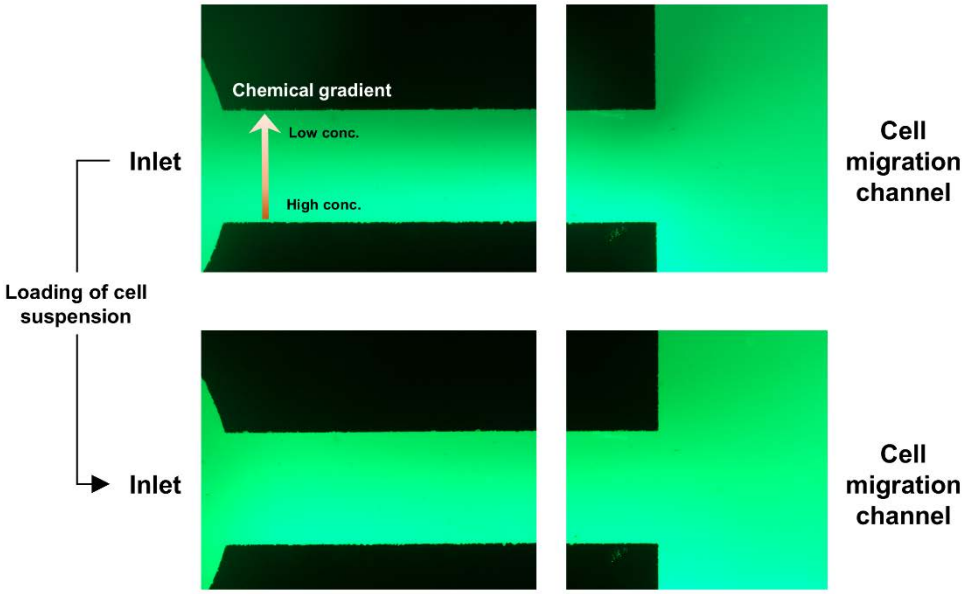

Figure S-1. Change of concentration gradients of fluorescein near the inlet and cell migration channel by loading of microalgal cell suspension.

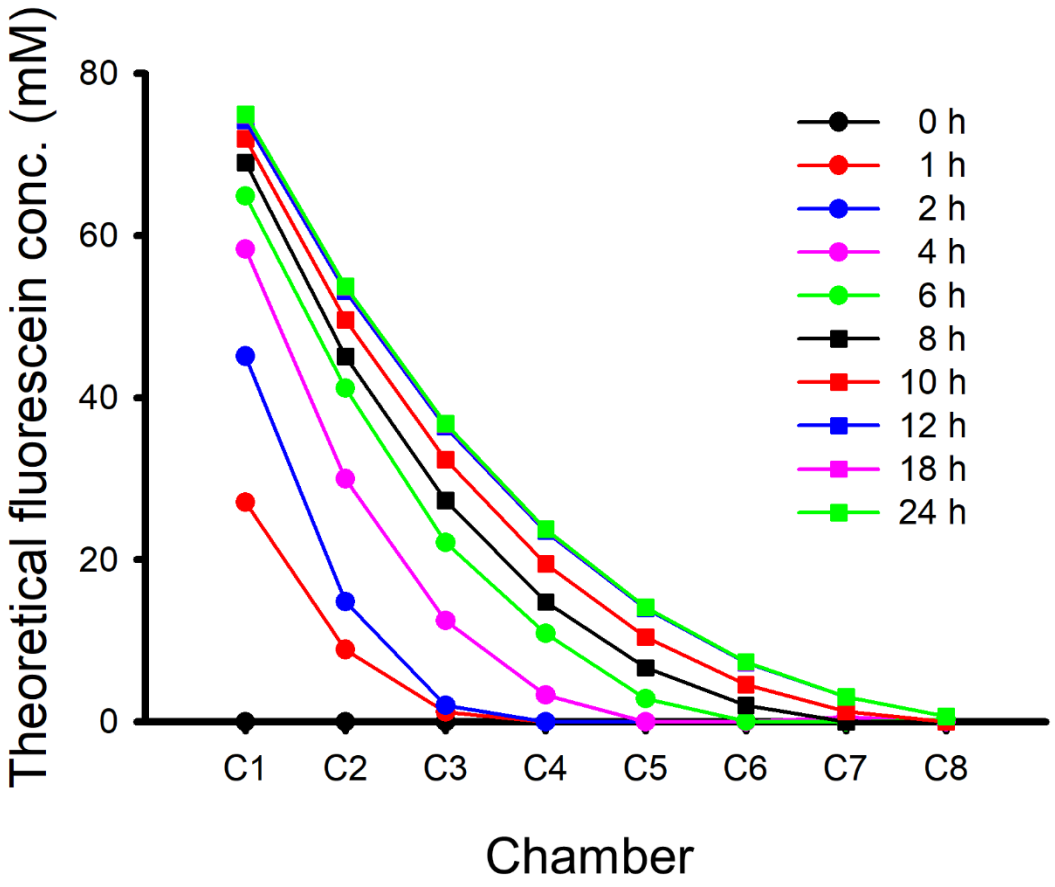

Figure S-2. Theoretical fluorescein concentration in the outlet chambers over time after loading in the chemical source reservoir.

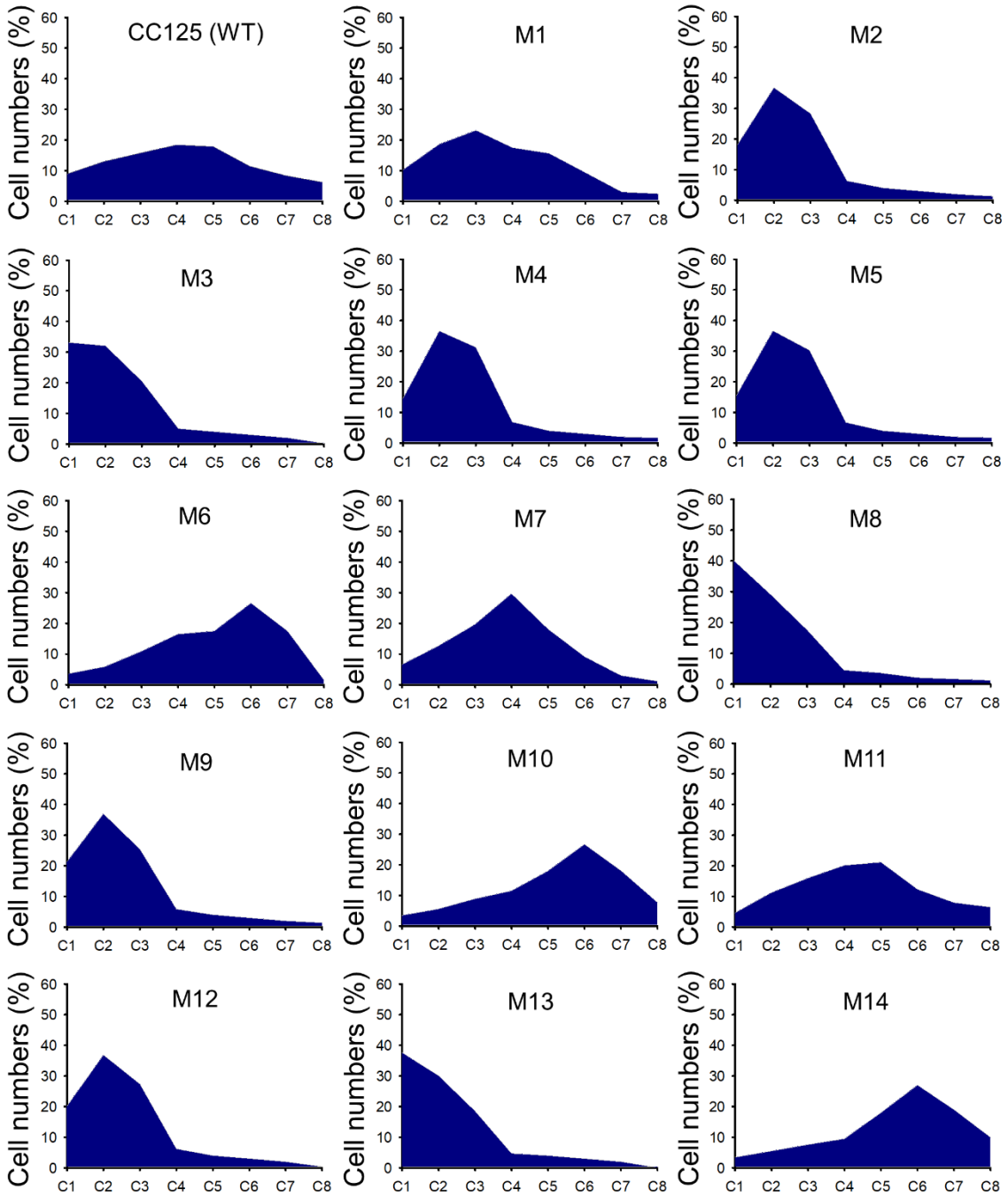

Figure S-3. Cell distribution histogram of wild type (CC125) and 14 insertional mutant strains in the two-dimensional microfluidic system.

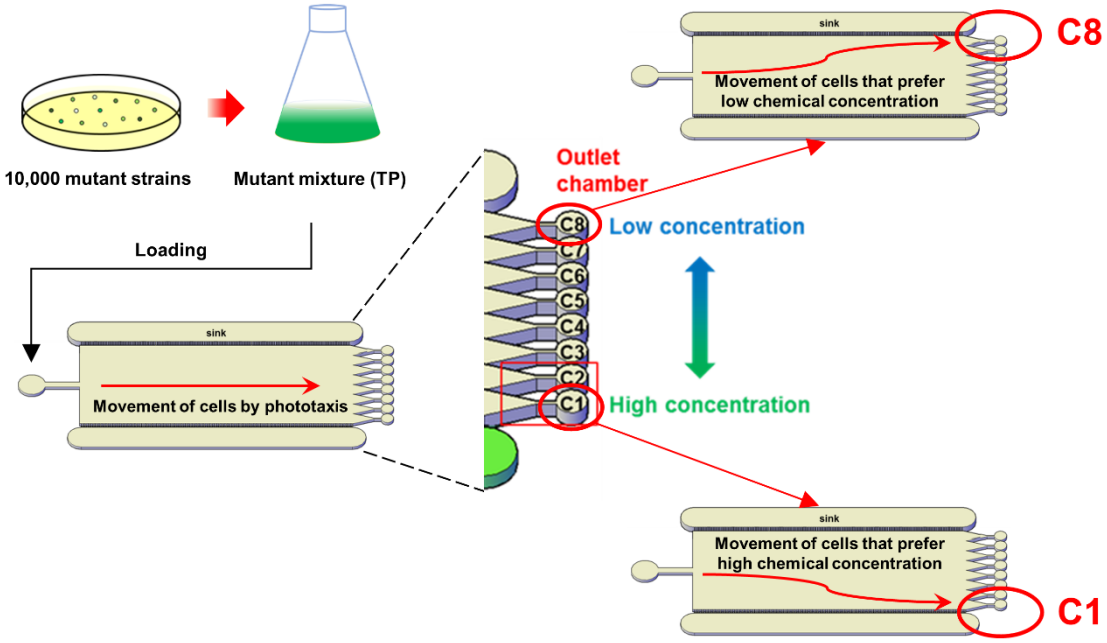

Figure S-4. Schematic diagram of the screening process for the isolation of mutant cell mixtures that showed different preferences for HCO_3^- concentration. The red arrows in microfluidics indicate the migration path of microalgae cells in the microfluidic channel. The microalgal cells moved towards the end of the cell migration channel along the *x*-axis by phototaxis and moved towards the outlet chambers along the *y*-axis by the HCO_3^- concentration preferred by the cells.

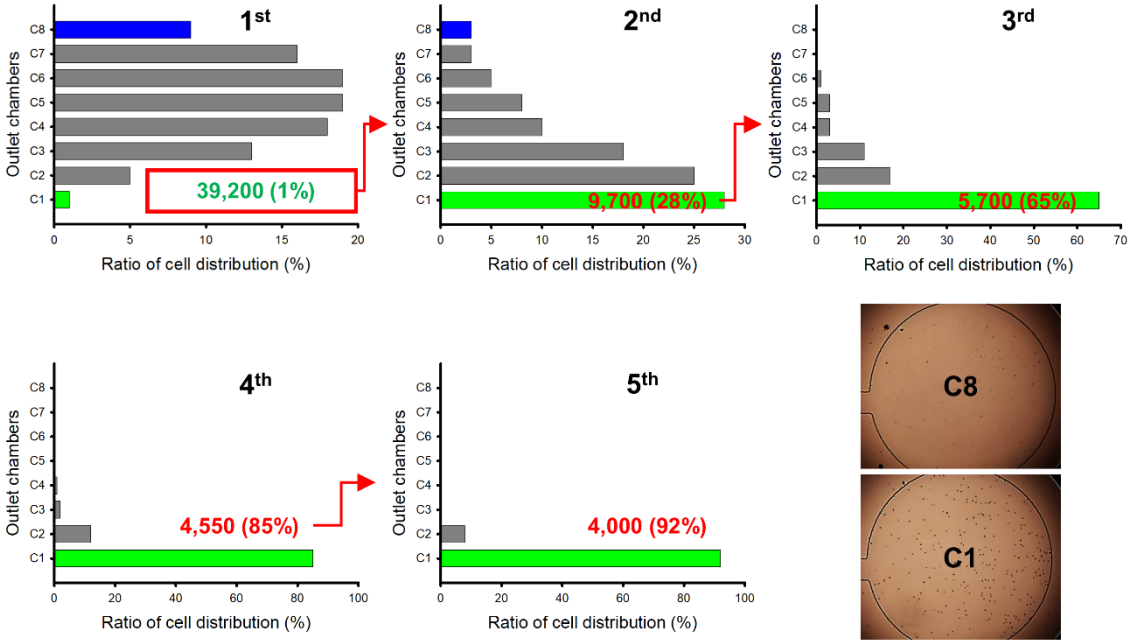

Figure S-5. Cell distribution in the outlet chambers of the microfluidic device during 5 consecutive high-throughput screenings to select cells with a strong chemotactic response to HCO_3^-. The separation efficiency during the screening process was expressed as the ratio of the number of cells reaching an outlet chamber C1 and the number of cells reaching all outlet chambers (C1 to C8).

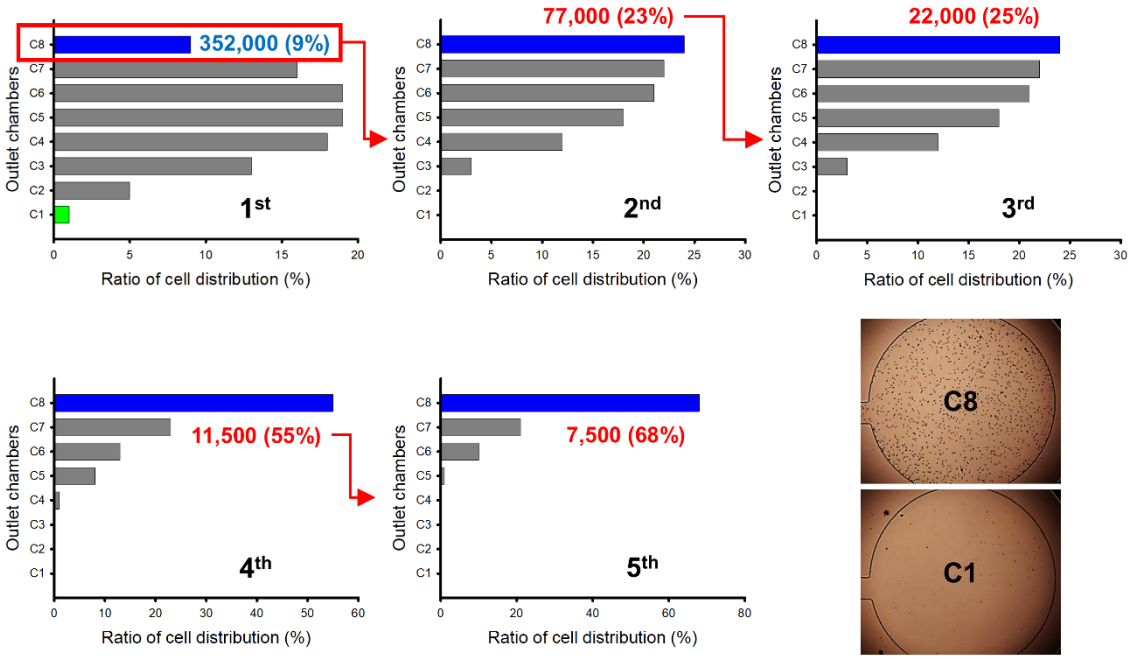

Figure S-6. Cell distribution in the outlet chambers of the microfluidic device during 5 consecutive high-throughput screenings to select cells with a weak chemotactic response to HCO_3^-. The separation efficiency during the screening process was expressed as the ratio of the number of cells reaching an outlet chamber C8 and the number of cells reaching all outlet chambers (C1 to C8).

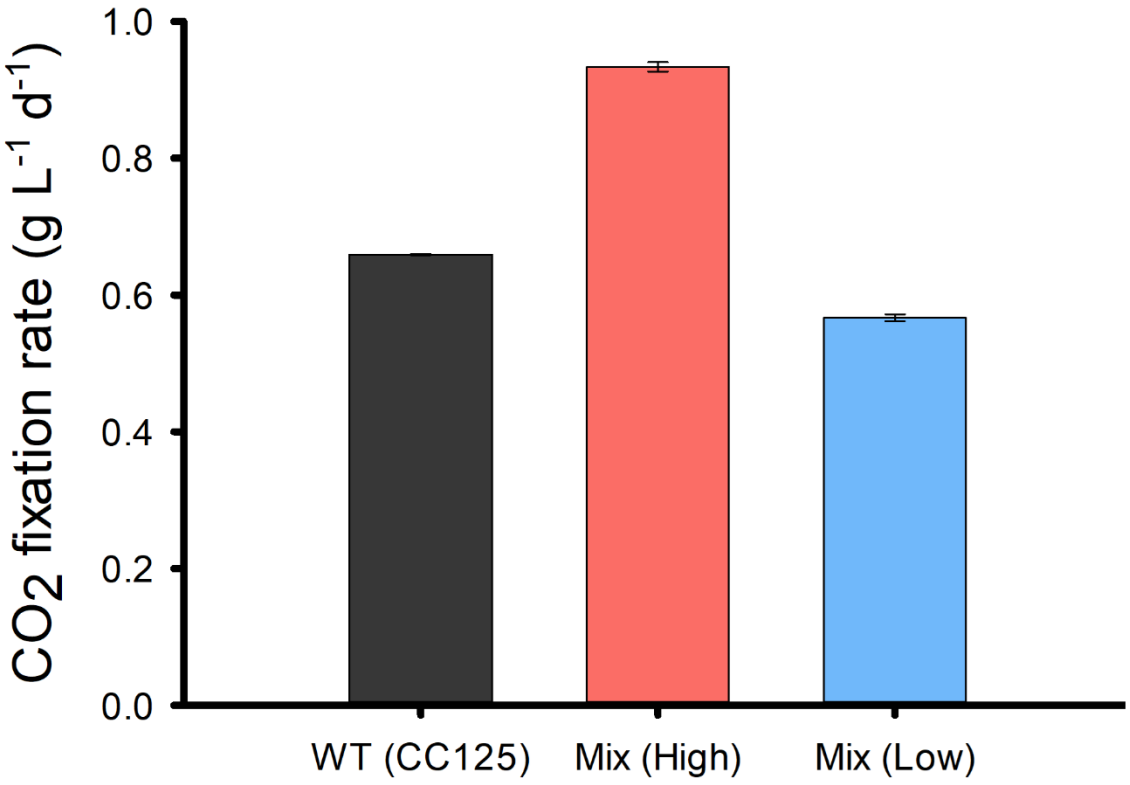

Figure S-7. The CO_2 fixation rate of the different microalgae strain groups photoautotrophically cultivated for 8 days.

References

1. Yun, Y. -S.; Lee, S. B.; Park, J. M.; Lee C. -I.; Yang, J. -W. Carbon Dioxide Fixation by Algal Cultivation Using Wastewater Nutrients. *J. Chem. Tech. Biotechnol.* **1997**, *69*, 451–455.

2. Tokarskyy, O.; Marshall, D. L. Mechanism of Synergistic Inhibition of *Listeria monocytogenes* Growth by Lactic Acid, Monolaurin, and Nisin. *Appl. Environ. Microbiol.* **2008**, *74*, 7126–7129.